

EXPERIMENTAL AND THEORETICAL STUDIES OF 4-[(4-METHYL-5-PHENYL-4H1,2,4-TRIAZOL-3-YL)SULFANYL]BENZENE-1,2-DICARBONITRILE

Ufuk Çoruh,^{1*} Reşat Ustabaş,² Hakkı Türker Akçay,³ Emre Mentеше,³ Ezequiel M. Vazquez Lopez⁴

¹Computer Education and Instructional Technology Department, Education Faculty, Ondokuz Mayıs University, 55200-Atakum-Samsun, Turkey

²Department of Middle Education, Education Faculty, Ondokuz Mayıs University, 55200-Atakum-Samsun, Turkey

³Department of Chemistry, Faculty of Sciences, Recep Tayyip Erdoğan University, 53100, Rize, Turkey

⁴Departamento de Química Inorgánica, Universidade de Vigo, Vigo 36310, Galicia, Spain

ucoruh@gmail.com

In this study, 4-[(4-methyl-5-phenyl-4H-1,2,4-triazol-3-yl)sulfanyl]benzene-1,2-dicarbonitrile was synthesized and its molecular structure was characterized by means of FT-IR and X-ray diffraction methods. The crystal is monoclinic and belongs to the P21/n space group. There are three weak intermolecular C-H...N type hydrogen bonds in the molecular structure. The geometrical parameters, vibration frequencies, HOMO–LUMO energies, and molecular electrostatic potential (MEP) map of the compound (3) in ground state were calculated by using density functional theory (DFT/B3LYP) with the 6-311G(d) basis set. Calculated geometrical parameters were compared with X-ray diffraction geometric parameters. On the other hand, theoretical and experimental FT-IR results were also compared.

Keywords: crystal structure; 1,2,4-triazole; DFT calculations; molecular electrostatic potential; frontier orbitals

ЕКСПЕРИМЕНТАЛНИ И ТЕОРЕТСКИ ИСПИТУВАЊА НА 4-[(4-МЕТИЛ-5-ФЕНИЛ-4H1,2,4-ТРИАЗОЛ-3-ИЛ)СУЛФАНИЛ]БЕНЗЕН-1,2-ДИКАРБОНИТРИЛ

Во ова истражување беше синтетизиран 4-[(4-метил-5-фенил-4H-1,2,4-триазол-3-ил)сулфанил]бензен-1,2-дикарбонитрил, а неговата структура беше карактеризирана со помош на FT-IR и рендгенска дифракција. Кристалот е моноклиничен и припаѓа на просторната група P21/n. Во молекулската структура постојат три слаби интермолекуларски водородни врски од типот на C-H...N. Геометриските параметри, вибрациските фреквенции, енергиите на HOMO–LUMO и мапата на молекулскиот електростатички потенцијал (MEP) на соединението (3) во основна состојба беа пресметани со теоријата на функционалот на густината (DFT/B3LYP) и основен сет 6-311G(d). Пресметаните геометриски параметри беа споредени со геометриските параметри добиени со рендгенската дифракција. Исто така беа споредени и теоретските и експерименталните резултати добиени со FT-IR.

Клучни зборови: кристална структура; 1,2,4-триазол; DFT пресметки; молекулски електростатички потенцијал; гранични орбитали

1. INTRODUCTION

1,2,4-triazoles, planar five-membered heterocyclic compounds with a 6π aromatic system, have an important role in synthetic chemistry. In particular, the pharmacological properties of this compound class have been extensively studied. It is known that these compounds show anti-inflammatory, antiviral, antimicrobial and antidepressant activities [1]. In addition, 1,2,4-triazole derivatives are potential chemosensors for the determination of many metal cations [2–11].

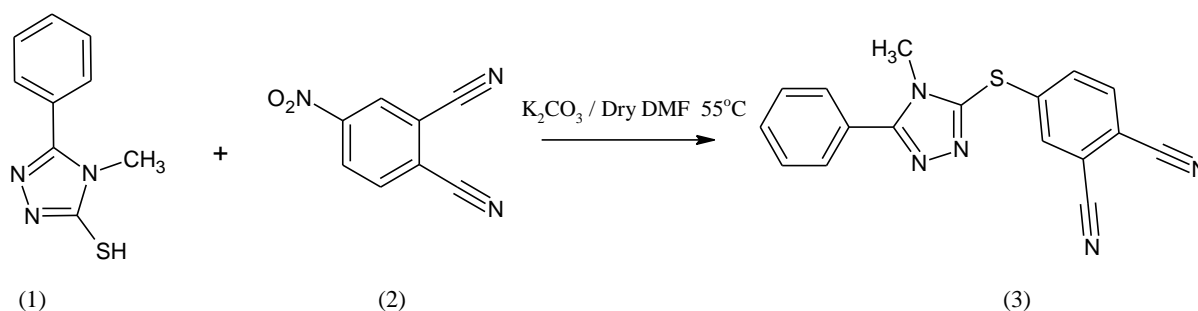
In this study, compound (3) was synthesized and its molecular structure was characterized by using FT-IR, X-ray diffraction, and quantum chemical methods. The geometrical parameters, vibration frequencies, molecular electrostatic potential, and frontier orbitals of compound (3) were calculated in the ground state by using DFT/B3LYP/6-311G(d). A comparison of the calculated geometric param-

eters with the experimental parameters of compound (3) was carried out.

2. EXPERIMENTAL SECTION

2.1. Synthesis

Dry DMF solution of 4-methyl-5-phenyl-4*H*-1,2,4-triazole-3-thiol (1) (0.61 g, 3.2 mmol) and 4-nitrophthalonitrile (2) (0.55 g, 3.2 mmol) were stirred for 10 min at 55 °C under N_2 atmosphere. Dry potassium carbonate (0.48 g, 3.5 mmol) was added to the reaction mixture for two hours and the reaction was conducted under N_2 atmosphere at 50 °C for 5 days. Then it was poured into ice-water. The creamy solid precipitate was filtered, washed with water, and dried in vacuum. Single crystals were obtained in acetone/petroleum ether solvent system. The yield was 0.71 g (70%).



Scheme 1. Synthesis route of compound (3)

2.2. Measurements and calculations

We used the Schlenk system, where all reactions were carried out under dry and oxygen-free nitrogen atmosphere. DMF (dimethylformamide) was dried and purified in accordance with the literature [12]. 4-methyl-5-phenyl-4*H*-1,2,4-triazole-3-thiol was prepared according to the literature [13]. A Perkin Elmer Spectrum One FT-IR device with the ATR technique was used for IR recordings. The X-ray data of compound (3) were measured on a Bruker Smart CCD area-detector diffractometer by using $CuK\alpha$ ($\lambda = 1.54178 \text{ \AA}$) X-rays. For data collection and cell refinement, the APEX2 [14] and Bruker SAINT [14] programs were used respectively. SHELXS-97 [15], SHELXL-97 [15], ORTEP III [16], and WinGX software [17] programs were used to solve and refine the structure, to define the molecular figures, and to prepare material for publication. Crystallographic data are given in Table 1.

All the theoretical calculations were performed by using the Gaussian 03 [18] program

package. The initial atomic coordinates of compound (3) were obtained by means of X-ray data. Via the GaussView [19] molecular visualization program, the geometry of the molecule in three dimensions was defined. DFT calculations were performed with the 6-311G(d) basis set by using B3LYP [20,21] (Becke's three-parameter hybrid functional using the LYP correlation functional) hybrid function. In order to calculate the vibration frequencies of the optimized structure, DFT/B3LYP methods and the 6-311G(d) basis set were used. The 0.9672 [22] scale value was used for the calculated vibration frequencies.

3. RESULTS AND DISCUSSION

3.1. Crystal structure

Compound (3) is a monoclinic system belonging to the $P21/n$ space group. The molecular structure of the title compound, which is obtained

by using the ORTEP-3 program, is shown in Figure 1. Furthermore, the packing diagram of compound (3) is given in Figure 2. The compound consists of one triazole and two benzene rings. When examining the bond lengths under the X-ray parameters of compound (3) in Table 3, it can be seen that especially C38-N32 [1.136 (2) Å], C37-N31 [1.144(2) Å], C3-S31[1.743 (2) Å], N1-N2

[1.381(2) Å], and N2-C3 [1.307(2) Å] are in conformity with the values in the literature [23–26]. The dihedral angles between the 1,2,4 triazole ring and the C31-C36 and C51-C56 rings are 76.92° and 27.53° respectively. The crystal structure has three weak intermolecular C-H...N type hydrogen bonds. The details related to these interactions are given in Table 2.

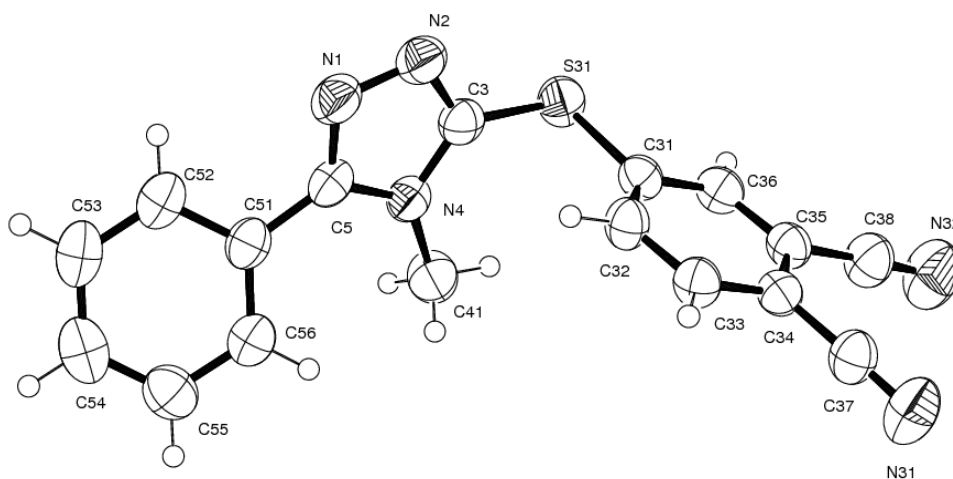


Fig. 1. Ortep-3 diagram of (3) with atom labeling

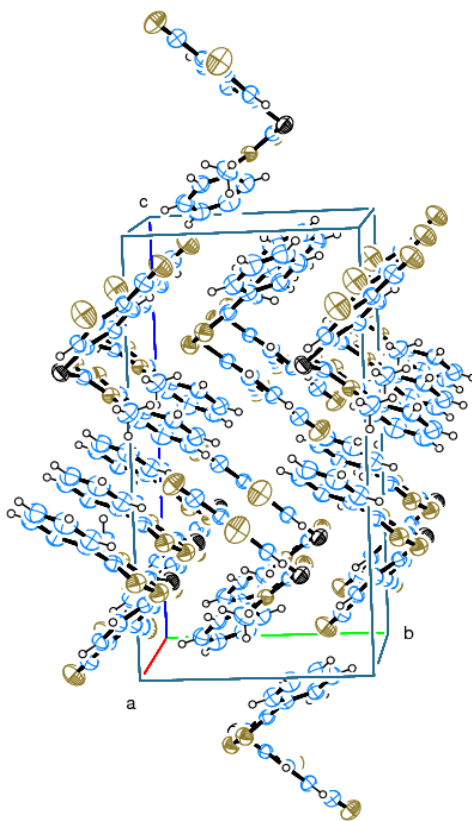


Fig. 2. Packing diagram of the title compound

Table 1

Crystallographic data for compound (3)

Chemical formula	C ₁₇ H ₁₁ N ₅ S
Formula weight	317.37
Crystal system	Monoclinic
Crystal shape/color	Prism/Colorless
Temperature (K)	293
Space group, Z	P2 ₁ /n, 4
a, b, c (Å)	8.3466(3), 9.8392(4), 18.6857(8)
β (°)	95.159(1)
V (Å ³)	1528.33(11)
D _x (Mg cm ⁻³)	1.379
Radiation type	CuKα
μ (mm ⁻¹)	1.929
F ₀₀₀	656
Crystal size (mm ³)	0.157×0.248×0.295
Data collection	
Diffractometer/meas.meth	Bruker CCD Smart /φ and ω-scans
Absorption correction	Multi-scan
T _{min} , T _{max}	0.4456, 0.7530
Number of measured, independent, and observed reflections	48158, 2779, 2673
Criterion for observed reflections	I > 2σ(I)
R _{int}	0.041
θ _{max}	68.22
Refinement	
Refinement on	F ²
R[F ² > 2σ(F ²)], wR, S	0.037, 0.109, 1.05
Number of reflections	2779
Number of parameters	209
Δρ _{max} , Δρ _{min} (eÅ ⁻³)	0.32, -0.24

Table 2

Hydrogen-bond geometry (Å, °)

D-H...A	D-H	H...A	D...A	D-H...A
C54-H54...N32 ⁱ	0.93(2)	2.93(2)	3.836(3)	163(1)
C53-H53...N31 ⁱ	0.93(2)	2.76(2)	3.452(2)	131(1)
C41-H41B...N31 ⁱⁱ	0.96(2)	2.70(2)	3.447(3)	134(1)

Symmetry code: (i) x-1/2-1, -y+1/2, z-1/2; (ii) x-1/2, -y+1/2, z-1/2

3.2. Optimized structures

In order to constitute the initial geometry of compound (3) for theoretical calculations, the experimental results of X-ray diffraction are used. To obtain the geometrical optimization of compound (3), the DFT/B3LYP method and 6-311G(d) basis set are used. Experimental and calculated geometrical parameters, bond lengths, bond angles, and torsion angles for compound (3) are given in Table 3. To compare the consistency of the calculated and experimental geometric parameters, the RMSE values are found. These values are 0.014 Å for bond lengths and 0.78° for bond angles. As can be seen in Table 3, the greatest deviations in C31-S31

bond length and C3-S31-C31 bond angles are found to be 0.032 Å and 1.27°.

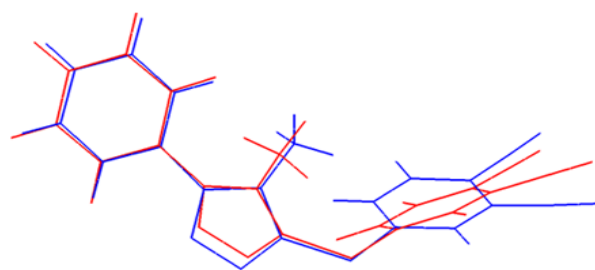


Fig. 3. Superposition of molecular conformation of (3) as established from X-ray (red) and DFT calculation (blue)

Table 3

Theoretical and experimental molecular structure parameters

	X-ray	B3LYP/6-311G(d)
Bond Lengths(Å)		
C38–N32	1.136	1.154
C37–N31	1.144	1.154
C34–C37	1.431	1.428
C35–C36	1.381	1.399
C31–C32	1.390	1.398
C31–S31	1.767	1.799
C3–S31	1.743	1.763
C3–N2	1.307	1.313
C3–N4	1.366	1.380
N4–C41	1.459	1.459
N4–C5	1.366	1.373
N1–C5	1.322	1.322
N1–N2	1.381	1.363
C5–C51	1.465	1.469
C51–C52	1.393	1.402
Bond angles (°)		
C55–C56–C51	120.32	120.38
C3–S31–C31	102.80	101.53
C3–N4–C5	104.77	104.04
C3–N4–C41	125.65	126.85
C5–N4–C41	129.58	128.96
N31–C37–C34	178.32	178.55
C32–C31–C36	120.30	120.06
C32–C31–S31	123.12	122.02
C36–C31–S31	116.57	117.80
C35–C36–C31	119.49	120.30
C5–N1–N2	108.16	108.18
N1–C5–N4	109.40	109.78
N1–C5–C51	123.55	123.48
N4–C5–C51	126.94	126.71
C3–N2–N1	106.51	107.52
N2–C3–N4	111.17	110.45
N2–C3–S31	123.87	124.90
N4–C3–S31	124.74	124.63
N32–C38–C35	177.20	178.41
Torsion angles (°)		
C51–C56–C55–C54	–1.7	–0.29
C3–S31–C31–C32	–14.0	–39.5
S31–C31–C32–C33	–177.0	–177.2
N2–N1–C5–N4	–0.07	0.01
N2–N1–C5–C51	–176.3	–178.6
C31–C32–C33–C34	0.0	1.1
N1–C5–C51–C56	–154.2	–143.8
N1–N2–C3–S31	174.8	179.6
C5–N4–C3–N2	0.0	–0.3

Furthermore, the superposition of the atomic positions of compound (3), which are obtained by theoretical and experimental methods, is shown in Figure 3. The RMSE value is calculated as 0.32 Å. The calculated dihedral angles between the 1,2,4 triazole ring and the C31–C36 and C51–C56 rings of the molecular structure that is formed after the optimization of compound (3) are 76.56° and 35.41° respectively. The theoretical and experimental values of the dihedral angles are close to each other

3.3. Vibrational spectra

Characteristic C–H stretching vibrations of aromatic structures are observed between 3000 and 3150 cm⁻¹. In this study, the vibrations observed at 3115 and 3077 cm⁻¹ are calculated to be at 3092 and 3084 cm⁻¹ and show good agreement with the literature. The C–H₃ stretching vibrations are observed at 3047 and 2923 cm⁻¹ in the experimental IR spectrum in accordance with the literature. Also, they are calculated to be at 3033 and 2961 cm⁻¹ [27–29]. C≡N stretching vibration in the phthalonitrile ring is seen expressly at 2200–2300 cm⁻¹ as a sharp peak. The theoretical C≡N stretching vibrations were calculated to be at 2265 and 2269 cm⁻¹ and were observed at 2231 cm⁻¹.

The reason why only one sharp peak was observed in the theoretical and experimental spectra may be due to two C≡N stretching vibrations that are very near to each other [30–32].

The bending vibrations that occur inside the aromatic and aliphatic planes given in the literature are in the range of 1480–1000 cm⁻¹. In our study, the vibrations observed at 1486–1079 cm⁻¹ are calculated to occur at 1480–1104 cm⁻¹ and are characterized as C–H bending vibrations in plane. All these results are in good agreement with the associated literature [30, 31, 33, 34].

The stretching vibrations $\nu(\text{C}=\text{C})$ and $\nu(\text{C}=\text{N})$ which belong to the phenyl and triazole groups were calculated to be at 1572, 1530, 1454, 1445, 1382, 1270, and 1196 cm⁻¹ and were observed at 1587, 1565, 1456, 1428, 1329, 1262, and 1206 cm⁻¹, in agreement with the literature [35–36].

The C–H out-of-plane bending wagging at the phenyl and triazole rings is observed at about 675–1000 cm⁻¹. In this study, the peaks calculated to be at 1104, 1085, 1010, 902, 837, 762, 712, and 687 cm⁻¹ are matched with the peaks observed at 1079, 1056, 991, 901, 853, 772, 719, and 693 cm⁻¹ and defined as wagging [30, 35, 36]. CCC (in-plane bending) vibration is observed at about 1000 cm⁻¹. We defined this vibration experimentally at 991 cm⁻¹ and also theoretically at 1010 cm⁻¹ [32, 37].

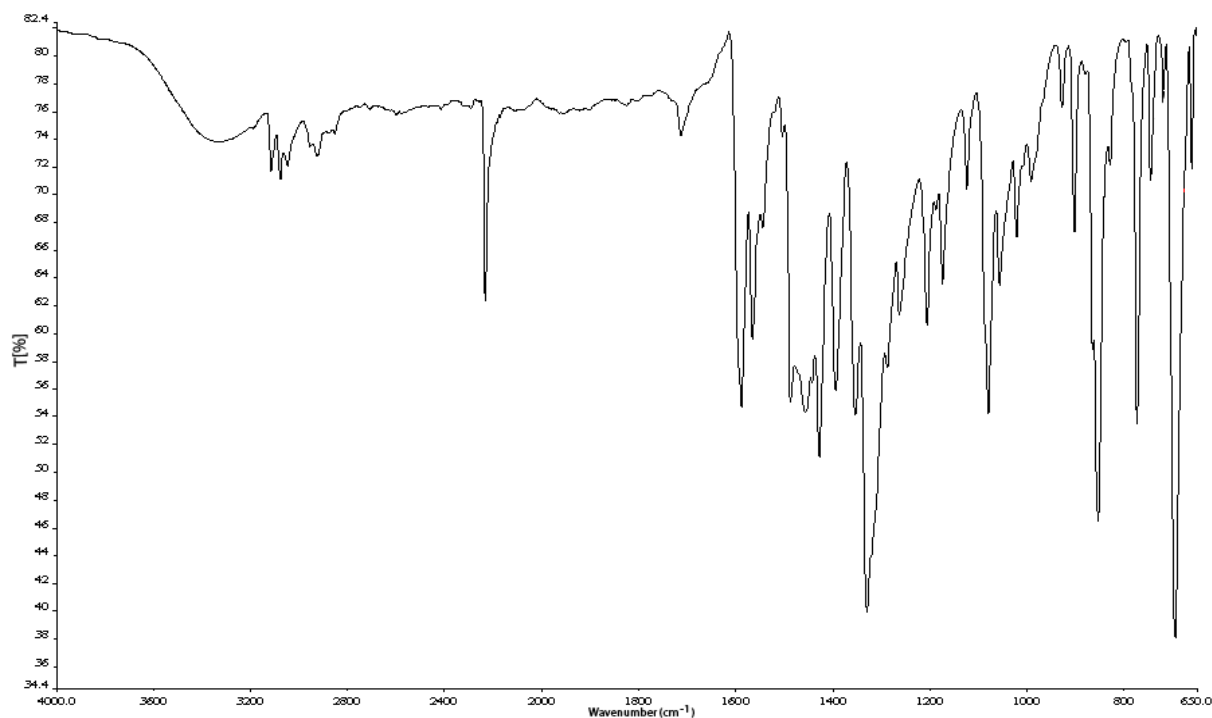


Fig. 4. Experimental IR spectrum of the compound (3)

Table 4

Values of the experimental and calculated vibrational frequencies (cm^{-1})

Assignments ^a	Experimental	Calculated
$\nu(\text{C-H})_s$	3115	3092
$\nu(\text{C-H})_s$	3077	3084
$\nu(\text{C-H}_3)_{as}$	3047	3033
$\nu(\text{C-H}_3)_s$	2923	2961
$\nu(\text{C}\equiv\text{N})_s$	2231	2265
$\nu(\text{C}=\text{C})$	1587	1572
$\nu(\text{C}=\text{C})$	1565	1530
$\gamma(\text{C-H}) + \omega(\text{C-H}_3)$	1486	1480
$\nu(\text{C}=\text{N}) + \gamma(\text{C-H}) + \omega(\text{C-H}_3)$	1456	1454
$\gamma(\text{C-H}) + \omega(\text{C-H}_3) + \nu(\text{C}-\text{C})$	1428	1445
$\gamma(\text{C-H}) + \omega(\text{C-H}_3)$	1394	1425
$\nu(\text{C}=\text{N}) + \nu(\text{C}-\text{N}) + \omega(\text{C-H}_3) + \gamma(\text{C-H})$	1329	1382
$\nu(\text{C}-\text{C})$	1262	1270
$\gamma(\text{C-H}) + \nu(\text{C}-\text{CN})$	1206	1196
$\gamma(\text{C-H})$	1174	1172
$\nu(\text{C}-\text{S}) + \omega(\text{C-H}_3) + \gamma(\text{C-H})$	1079	1104
$\nu(\text{N}-\text{N}) + \omega(\text{C-H}_3)$	1056	1085
$\nu(\text{C}-\text{S})$	1021	1061
$\beta(\text{CCC}) + \omega(\text{C-H}_3)$	991	1010
$\omega(\text{C-H})$	901	902
$\omega(\text{C-H})$	853	837
$\omega(\text{C-H}) + \tau(\text{CCCN})$	772	762
$\omega(\text{C-H}) + \tau(\text{CCNN})$	719	712
$\omega(\text{C-H})$	693	687

^a ν , stretching; γ , rocking; ω , wagging; β , bending; τ , torsion; s, symmetric; as, asymmetric

3.4. Frontier molecular orbital and molecular electrostatic potential

By means of the DFT/B3LYP method applied on the optimized structure derived from the 6-311G(d) basis set, the frontier molecular orbitals and MEP map are obtained. As can be seen in Figure 5, the HOMO is generally concentrated on the 1,2,4 triazole and phenyl rings. On the other hand, LUMO is concentrated on the phthalonitriles ring system. HOMO and LUMO have energy levels of -7.08 and -2.69 eV respectively. $\text{Gap} = E_{\text{HOMO}} - E_{\text{LUMO}}$, and hardness = $\text{Gap}/2$ [38]. The HOMO–LUMO energy difference is 4.39 eV and the hardness of the molecule corresponds to 2.19 eV.

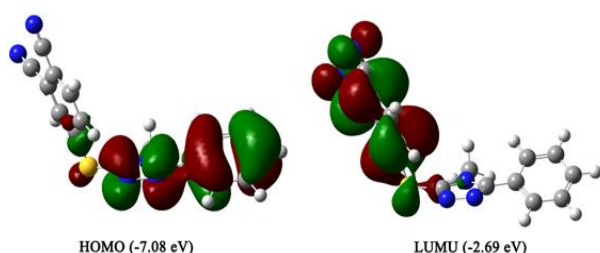


Fig. 5. Molecular orbital surfaces and energy levels using the DFT/B3LYP method for the HOMO and LUMO of compound (3)

The molecular electrostatic potential (MEP) is calculated considering the electrical charge of the related molecule. We can define electronegative and electropositive locations looking at these results as well as hydrogen bonding interactions [39–41]. The MEP map of compound (3) is shown in Figure 6.

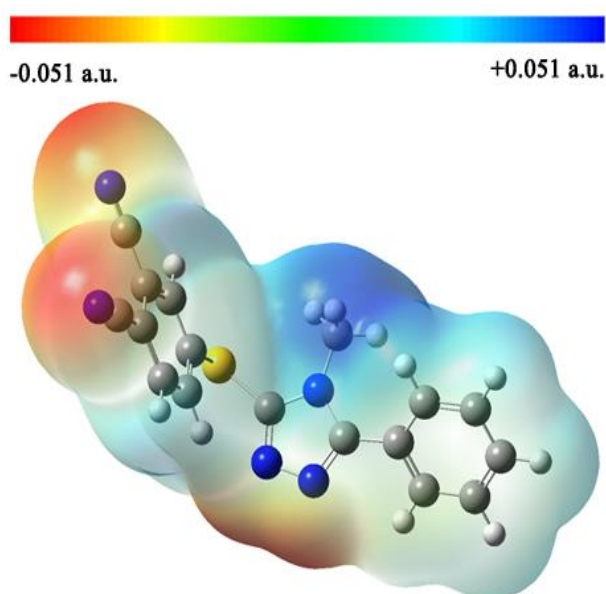


Fig. 6. Appearance of the molecular electrostatic potential (MEP) map of compound (3)

When examining the map, it can easily be seen that negative (red) partitions are mainly concentrated on cyano groups and on N1 and N2 atoms of the 1,2,4 triazole ring. These negative $V(r)$ values are -0.05 a.u. for N31, -0.048 a.u. for N32, -0.049 a.u. for N1, and -0.048 a.u. for N2. The largest positive (blue) partition is located around the methyl group and its $V(r)$ value is 0.038 a.u.

The MEP map provides the information that the molecular interactions will take place in these regions. Examining Table 2, this prediction about the interaction locations can be confirmed.

4. CONCLUSIONS

4-[(4-methyl-5-phenyl-4H-1,2,4-triazol-3-yl)sulfanyl]benzene-1,2-dicarbonitrile(3), formulated as C₁₇H₁₁N₅S, was synthesized and its molecular structure was characterized by means of FT-IR and X-ray diffraction methods. The calculated geometrical parameters in ground state obtained via the DFT/ B3LYP method with the 6-311G(d) basis set were compared with geometric parameters obtained via the X-ray diffraction experimental method and a very small difference was observed. Some small differences between theoretical calculations and experimental results are seen because the theoretical methods used consider a molecule alone unless there are interactions between neighbouring molecules in crystal form. Also, the experimental and calculated vibration frequencies were compared with each other and were found to be in compliance. The HOMO–LUMO energy gap was calculated as 4.39 eV.

Supplementary data

Further information can be obtained from the Cambridge Crystallographic Data Centre (E-mail:deposit@ccdc.cam.ac.uk), where the crystal structure X-ray data of compound (3) are stored under depository number CCDC-1441403.

Acknowledgement. The author would like to thank the Higher Education Council for supporting this study within international research.

REFERENCES

- [1] A. K. Srivastava, A. Kumar, N. Misra, P. S. Manjula, B. K. Sarojini, B. Narayana, Synthesis, spectral (FT-IR, UV-visible, NMR) features, biological activity prediction and theoretical studies of 4-Amino-3-(4-hydroxybenzyl)-1H-1,2,4-triazole-5(4H)-thione and its tautomer, *Journal of Molecular Structure*, **1107**, 137–144 (2016).

- [2] J.-L. Zhao, H. Tomiyasu, C. Wu, H. Cong, X. Zeng, S. Rahman, P. E. Georghiou, D. L. Hughes, C. Redshaw, T. Yamato, Synthesis, crystal structure and complexation behaviour study of an efficient Cu²⁺ ratiometric fluorescent chemosensor based on thiacalix[4]arene, *Tetrahedron*, **71**, 8521–8527 (2015)
- [3] A. N. Gusev, V. F. Shulgin, S. B. Meshkova, S. S. Smola, W. Linert, A novel triazole- based fluorescent chemosensor for zinc ions, *Journal of Luminescence*, **155**, 311–316 (2014).
- [4] J. Zhang, C. Yu, S. Qian, G. Lu, J. Chen, A selective fluorescent chemosensor with 1,2,4-triazole as subunit for Cu(II) and its application in imaging Cu(II) in living cells, *Dyes and Pigments*, **92**, 1370–1375 (2012).
- [5] D. Mandal, A. Thakur, S. Ghosh, A triazole tethered triferrocene derivative as a selective chemosensor for mercury(II) in aqueous environment, *Polyhedron*, **52**, 1109–1117 (2013).
- [6] N.-J. Wang, C.-M. Sun, W.-S. Chung, A specific and ratiometric chemosensor for Hg²⁺ based on triazole coupled ortho-methoxyphenylazocalix[4]arene, *Tetrahedron*, **67**, 8131–8139 (2011).
- [7] Y.-J. Zhang, X.-P. He, M. Hu, Z. Li, X.-X. Shi, G.-R. Chen, Highly optically selective and electrochemically active chemosensor for copper(II) based on triazole-linked glucosyl anthraquinone, *Dyes and Pigments*, **88**, 391–395 (2011).
- [8] T.-J. Jia, W. Cao, X.-J. Zheng, L.-P. Jin, A turn-on chemosensor based on naphthol–triazole for Al(III) and its application in bioimaging, *Tetrahedron Letters*, **54**, 3471–3474 (2013).
- [9] S. Joshi, S. Kumari, R. Bhattacharjee, A. Sarmah, R. Sakhuja, D. D. Pant, Experimental and theoretical study: Determination of dipole moment of synthesized coumarin-triazole derivatives and application as turn off fluorescence sensor: High sensitivity for iron(III) ions, *Sensors and Actuators B: Chemical*, **220**, 1266–1278 (2015).
- [10] N.-J. Wang, C.-M. Sun, W.-S. Chung, A highly selective fluorescent chemosensor for Ag⁺ based on calix[4]arene with lower-rim proximal triazolylpyrenes, *Sensors and Actuators B: Chemical*, **171–172**, 984–993 (2012).
- [11] J.-H. Ye, J. L. Z. Wang, Y. Bai, W. Zhang, W. He, A new Fe³⁺ fluorescent chemosensor based on aggregation-induced emission, *Tetrahedron Letters*, **55**, 3688–3692 (2014).
- [12] D. D. Perin, W. L. F. Armarego, *Purification of laboratory chemicals*, Pergamon, Oxford, 1989.
- [13] J. M. Kane, M. A. Staeger, C. R. Dalton, F. P. Miller, M. W. Dudley, A. M. L. Ogden, J. H. Kehne, H. J. Ketteler, T. C. McCloskey, Y. Senyah, P. A. Chmielewski, J. A. Miller, 5-Aryl-3-(alkylthio)-4H- 1,2,4-triazoles as Selective Antagonists of Strychnine-Induced Convulsions and Potential Antispastic Agents, *J. Med. Chem.*, **37**, 125–132 (1994).
- [14] Bruker (2009). APEX2 and SAINT. Bruker AXS Inc., Madison, Wisconsin, USA.
- [15] G. M. Sheldrick, *SHELXS97 and SHELXL97*, University of Göttingen, Germany, 1997.
- [16] L. J. Farrugia, ORTEP-3 for Windows – A version of ORTEP-III with a Graphical User Interface (GUI), *J. Appl. Cryst.*, **30**, 565 (1997).
- [17] L. J. Farrugia, WinGX suite for small-molecule single-crystal crystallography, *J. Appl. Cryst.*, **32**, 837–838 (1999).
- [18] M. J. Frisch, G. W. Trucks, H. B. Schlegel, G. E. Scuseria, M. A. Robb, J. R. Cheeseman, J. A. Montgomery Jr., J. T. Vreven, K. N. Kudin, J. C. Burant, J. M. Millam, S. S. Iyengar, J. Tomasi, V. Barone, B. Mennucci, M. Cossi, G. Scalmani, N. Rega, G. A. Petersson, H. Nakatsuji, M. Hada, M. Ehara, K. Toyota, R. Fukuda, J. Hasegawa, M. Ishida, T. Nakajima, Y. Honda, O. Kitao, H. Nakai, M. Klene, X. Li, J. E. Knox, H. P. Hratchian, J. B. Cross, V. Bakken, C. Adamo, J. Jaramillo, R. Gomperts, R. E. Stratmann, O. Yazyev, A. J. Austin, R. Cammi, C. Pomelli, J. W. Ochterski, P. Y. Ayala, K. Morokuma, G. A. Voth, P. Salvador, J. J. Dannenberg, V. G. Zakrzewski, S. Dapprich, A. D. Daniels, M. C. Strain, O. Farkas, D. K. Malick, A. D. Rabuck, K. Raghavachari, J. B. Foresman, J. V. Ortiz, Q. Cui, A. G. Baboul, S. Clifford, J. Cioslowski, B. B. Stefanov, G. Lui, A. Liashenko, P. Piskorz, I. Komaromi, R. L. Martin, D. J. Fox, T. Keith, M. A. Al-Laham, C. Y. Peng, A. Nanayakkara, M. Challacombe, P. M. W. B. Gill, B. Johnson, W. Chen, M. W. Wong, C. Gonzalez, J. A. Pople, *GAUSSIAN 03, Revision E.01*, Gaussian Inc., Wallingford CT, 2004.
- [19] R. Dennington II, T. Keith, J. Millam, *Gauss View Version 4.1 2*, Semichem, Inc., Shawnee Mission, KS, 2007.
- [20] P. J. Stephens, F. J. Devlin, C. F. Chablowski, M. J. Frisch, Ab Initio Calculation of Vibrational Absorption and Circular Dichroism Spectra Using Density Functional Force Fields, *J. Phys. Chem.*, **98**, 11623–11627 (1994).
- [21] C. Peng, P. Y. Ayala, H. B. Schlegel, M. J. Frisch, Using redundant internal coordinates to optimize equilibrium geometries and transition states, *J. Comput. Chem.*, **17**, 49–56 (1996).
- [22] J. P. Merrick, D. Moran, L. Radom, An Evaluation of Harmonic Vibrational Frequency Scale Factors, *J. Phys. Chem.*, **A 111**, 11683–11700 (2007).
- [23] H. K. Fun, M. Hemamalini, N. Kalluraya, B. Kalluraya, 4-([4-Amino-5-(4-chloroanilino)methyl]-4H-1,2,4-triazol-3-yl)sulfanyl)acetyl)-3-(4-methoxyphenyl)-1,2,3-oxadiazol-3-ium-5-olate, *Acta Cryst.* **E66**, o3178 (2010)
- [24] H. T. Akçay, R. Bayrak, E. Şahin, K. Karaoğlu, Ü. Demirbaş, Experimental and computational studies on 4-[(3,5-dimethyl-1H-pyrazol-1-yl)methoxy]phthalonitrile and synthesis and spectroscopic characterization of its novel phthalocyanine magnesium(II) and tin(II) metal complexes, *Spectrochimica Acta, Part A: Molecular and Biomolecular Spectroscopy*, **114**, 531–540 (2013).
- [25] A. A. El-Emam, S. Lahsani, H. H. Asiri, C. K. Quah, H. K. Fun, 2-([5-(Adamantan-1-yl)-4-methyl-4H- 1,2,4-triazol-3-yl)sulfanyl]-N,N-dimethylethanamine, *Acta Cryst.*, **E67**, o1356(2012).
- [26] H. Tuncer, A. O. Görgülü, T. Hökelek, 4-(Furan-2-ylmethoxy)benzene-1,2-dicarbonitrile, *Acta Cryst.* **E68**, o153 (2012).

- [27] A. A. El-Emam, A-M. S. Al-Tamimi, K. A. Al-Rashood, H. N. Misra, V. Narayan, O. Prasad, L. Sinha, Structural and spectroscopic characterization of a novel potential chemotherapeutic agent 3-(1-adamantyl)-1-[[4-(2-methoxyphenyl)piperazin-1-yl]methyl]-4-methyl-1H-1,2,4-triazole-5(4H)-thione by first principle calculations, *Journal of Molecular Structure*, **1022**, 49–60 (2012).
- [28] M. Koparir, C. Orek, P. Koparir, K. Sarac, Synthesis, experimental, theoretical characterization and biological activities of 4-ethyl-5-(2-hydroxyphenyl)-2H-1,2,4-triazole-3(4H)-thione, *Spectrochimica Acta Part A: Molecular and Biomolecular Spectroscopy*, **105**, 522–531 (2013).
- [29] E. Düğdü, Y. Ünver, D. Ünlüer, H. Tanak, K. Sancak, Y. Köysal, Ş. Işık, Synthesis, structural characterization and comparison of experimental and theoretical results by DFT level of molecular structure of 4-(4-methoxyphenethyl)-3,5-dimethyl-4H-1,2,4-Triazole, *Spectrochimica Acta Part A: Molecular and Biomolecular Spectroscopy*, **108**, 329–337 (2013).
- [30] H. T. Akçay, R. Bayrak, S. Karşlıoğlu, E. Sahin, Synthesis, characterization and spectroscopic studies of novel peripherally tetra-imidazole substituted phthalocyanine and its metal complexes, the computational and experimental studies of the novel phthalonitrile derivative, *Journal of Organometallic Chemistry*, **713**, 1–10 (2012).
- [31] H. T. Akçay, R. Bayrak, E. Sahin, K. Karaoglu, U. Demirbas, Experimental and computational studies on 4-[(3,5-dimethyl-1H-pyrazol-1-yl)methoxy]phthalonitrile and synthesis and spectroscopic characterization of its novel phthalocyanine magnesium(II) and tin(II) metal complexes, *Spectrochimica Acta Part A: Molecular and Biomolecular Spectroscopy*, **114**, 531–540 (2013).
- [32] A. Coruh, F. Yılmaz, B. Sengez, M. Kurt, M. Cinar, M. Karabacak, Synthesis, molecular conformation, vibrational, electronic transition, and chemical shift assignments of 4-(thiophene-3-ylmethoxy)phthalonitrile: a combined experimental and theoretical analysis, *Struct. Chem.*, **22**, 45–56 (2011).
- [33] M. Karabacak, Z. Cinar, M. Kurt, S. Sudha, N. Sundaraganesan, FT-IR, FT-Raman, NMR and UV-vis spectra, vibrational assignments and DFT calculations of 4-butyl benzoic acid, *Spectrochim. Acta A*, **85**, 179–189 (2012).
- [34] S. Muthu, E. E. Porchelvi, Experimental spectroscopic (FTIR, FT-Raman, FT-NMR, UV-Visible) and DFT studies of 1-ethyl-1,4-dihydro-7-methyl-4oxo-1,8 naphthyridine-3-carboxylic acids, *Spectrochim. Acta A*, **116**, 220–235 (2013).
- [35] H. T. Akçay, R. Bayrak, Computational studies on the anastrozole and letrozole, effective chemotherapy drugs against breast cancer, *Spectrochimica Acta, Part A: Molecular and Biomolecular Spectroscopy*, **122**, 142–152 (2014).
- [36] S. Qiu, J. Wei, F. Pan, J. Liu, A. Zhang, Vibrational, NMR spectrum and orbital analysis of 3,3',5,5'-tetrabromobisphenol A: A combined experimental and computational study, *Spectrochim. Acta A*, **105**, 38–44 (2013).
- [37] M. Kandasamy, G. Velraj, S. Kalaichelvan, Vibrational spectra, NMR and HOMO-LUMO analysis of 9-fluorenone-2-carboxylic acid, *Spectrochim. Acta A*, **105**, 176–183(2013).
- [38] Pearson, R. G, Density functional theory-electronegativity and hardness chemtracts, *Inorg. chem.*, **3**, 317–333 (1991).
- [39] E. Scrocco, J. Tomasi, Electronic Molecular Structure, Reactivity and Intermolecular Forces: An Euristic Interpretation by Means of Electrostatic Molecular Potentials, *Adv. Quant. Chem.*, **11**, 115–193 (1979).
- [40] F. J. Luque, J. M. Lopez, M. Orozco, Perspective on Electrostatic interactions of a solute with a continuum. A direct utilization of ab initio molecular potentials for the prevision of solvent effects, *Theor. Chem. Acc.*, **103**, 343–345(2000).
- [41] N. Okulik, A. H. Jubert, Internet Electron. *J. Mol. Des.*, **4**, 17–30(2005).

